Immunotoxic Effects of Perfluorononanoic Acid on BALB/c Mice

Xuemei Fang,*,† Lianjun Zhang,‡ Yixing Feng,* Yong Zhao,‡ and Jiayin Dai*,1

*Key Laboratory of Animal Ecology and Conservation Biology, Institute of Zoology, Chinese Academy of Sciences, Beijing 100190, China; †Graduate School of the Chinese Academy of Sciences, Beijing 100080, China; and ‡State Key Laboratory of Biomembrane and Membrane Biotechnology, Institute of Zoology, Chinese Academy of Sciences, Beijing 100190, China

The effects of perfluorononanoic acid (PFNA) on the immune system and its mechanism of action in mice have not been elucidated. Thus, BALB/c mice were exposed to the PFNA (0, 1, 3, or 5 mg/kg/day) for fourteen days. Exposure to PFNA led to a decrease in body weight and in the weight of the lymphoid organs. Cell cycle arrest and apoptosis were observed in the spleen and thymus following PFNA exposure. In the thymus, PFNA mostly modulated $CD4^+CD8^+$ thymocytes, whereas the $F4/80^+$, $CD11c^+$, and $CD49b^+$ cells were major targets in the spleen. Although concanavalin A–induced T lymphocyte blastogenesis was not altered by PFNA, production of interleukin (IL)-4 and interferon-gamma by splenic lymphocytes was remarkably impaired. The levels of cortisol and adrenocorticotrophic hormone in sera were increased; however, the expression of glucocorticoid receptor in the thymus was unchanged. In addition, expression of the peroxisome proliferator–activated receptors (PPAR-α and PPAR-γ) and IL-1β were upregulated significantly in the thymus at a dose of 1 mg PFNA/kg/day. No significant changes in expression of the inhibitory protein IκBα and IκBα kinase were observed. Together, these results suggest that PFNA exerts toxic effects on lymphoid organs and T cell and innate immune cell homeostasis in mice and that these effects may result from the activation of PPAR-α, PPAR-γ, and the hypothalamic-pituitary-adrenal axis. Interestingly, at the transcriptional level, the nuclear factor-kappa B signaling pathway appears to be uninvolved in the immunotoxic potential of PFNA.

Key Words: PFNA; Immunotoxicity; PPAR; glucocorticoid; NF-κB.

In recent years, concern about perfluorinated compounds (PFCs), a class of widespread environmental contaminants, has grown. The high-energy carbon-fluorine (C–F) bond renders these compounds resistant to hydrolysis, photolysis, microbial degradation, and metabolism by animals, and thus, makes these compounds environmentally persistent and poorly eliminated once absorbed (Giesy and Kannan, 2002). PFCs are bi-ologically active and have been reported to cause hepatotoxicity, developmental toxicity, reproductive toxicity, and endocrine toxicity (Lau *et al.*, 2007). Although a few studies have assessed immune modulation following exposure to PFCs (DeWitt *et al.*, 2008; Nelson *et al.*, 1992; Peden-Adams *et al.*, 2007, 2008; Yang *et al.*, 2000, 2001, 2002), the results were not entirely consistent due, in part, to the different methods and compounds investigated. Furthermore, the modes of action of these compounds have not yet been elucidated. Some studies have focused on peroxisome proliferator–activated receptors (PPARs) agonism to postulate the mechanism of immunotoxicity because PFCs are peroxisome proliferating chemicals (PPCs) (Yang *et al.*, 2002). PPARs were once believed to predominantly regulate genes associated with lipid metabolism; however, the roles of PPARs in the regulation of inflammation and immunity are rapidly evolving. PPARs bind the retinoid receptor RXR and regulate gene expression by binding to specific DNA sequence elements termed PPAR response elements (Tugwood *et al.*, 1992). PPAR agonists may exert anti-inflammatory and immunomodulatory actions through a DNA binding-independent interference of transcription factor pathways, such as nuclear factor-kappa B (NF-κB) signaling pathway (Delerive *et al.*, 2000) and activator protein-1 (AP-1) signaling pathway (Ricote *et al.*, 1998).

Glucocorticoids (GCs), which are mainly composed of cortisol and corticosterone, are the end-effectors of the hypothalamic-pituitary-adrenal (HPA) axis. GCs play important roles in the process of immunomodulation (Jondal *et al.*, 2004). Exposure to environmental chemicals, such as polychlorinated biphenyls, polycyclic aromatic hydrocarbons, 2,3,7,8-tetrachlorodibenzo-*p*-dioxin, and heavy metals, can alter the secretion of GCs and, thus, influence the immune system (Love *et al.*, 2003; Pabello and Lawrence, 2006; Rice and Hayward, 1997; Shridhar *et al.*, 2001). Previous studies implicated GCs in the mechanism of the anti-inflammatory effect of some PPAR agonists (Ialenti *et al.*, 2005). In Sprague-Dawley rats, for instance, the level of corticosterone in the blood was increased significantly by fenofibrate, a PPAR-α agonist (Chen *et al.*, 2008). Therefore, exposure to PFCs may affect the secretion of GCs in mice, and alterations in GCs level will result in immunomodulation.

[1] To whom correspondence should be addressed at Key Laboratory of Animal Ecology and Conservation Biology, Institute of Zoology, Chinese Academy of Sciences, Beijing, 100101, China. Fax: +86-10-64807099. E-mail: daijy@ioz.ac.cn.

To date, most toxicological studies of PFCs have been focused on perfluorooctanoic acid (PFOA) and perfluorooctane sulfonate (PFOS), and only a few studies have reported on the toxicity of PFNA, a compound with a nine-carbon length (Kleszczyński *et al.*, 2007; Kudo *et al.*, 2006). PFNA can be bioaccumulated and biomagnified through food webs and it have shown potentials for reproductive interference in animal experiments (Houde *et al.*, 2006). Several studies have reported the presence of PFNA in a variety of wildlife species, including, amphipod, fish, birds, and mammals (Haukas *et al.*, 2007; Van de Vijver *et al.*, 2005). Human contamination by PFNA has been reported in blood and seminal plasma and the highest concentration of PFNA (0.47 ng/ml) was reported in blood serum of urban tea worker populations in Sri Lanka (Guruge *et al.*, 2005). In many cases, the source and mode of transmission of PFCs to wildlife is unknown. However, a likely source is atmospheric fluorotelomer alcohol, which is emitted through industrial activities and produces perfluorinated carboxylic acids upon degradation (Ellis, *et al.*, 2004). As little is known about the immunotoxicity of PFNA, the aim of this study was to investigate the immunotoxicity of PFNA in BALB/c mice and to evaluate the mechanism of this immunotoxicity by exploring the possible involvement of PPARs, NF-κB–signaling pathways, and the HPA axis.

MATERIALS AND METHODS

Animals and treatment. Male BALB/c mice (Weitong Lihua Experimentary Animal Center, Beijing, China) were maintained in a pathogen-free facility and used at 6–8 weeks of age. Mice were randomly housed in four groups in microisolator cages containing sterilized feed and autoclaved bedding. After acclimatization for one week, the four groups of mice ($n = 6$) were treated with different doses of PFNA (0, 1, 3, and 5 mg/kg) via gastric gavage once a day for fourteen days. The doses were based on a preliminary trial in which half of the mice died during treatment for fourteen days with a dose of 10 mg PFNA/kg/day. Following treatment, the mice were weighed each day. All mice were sacrificed by cervical dislocation at the end of fourteen days experiment. Blood was collected before sacrifice according to the previous study (Preil *et al.*, 2001). Briefly, blood samples were obtained rapidly from the retroorbital sinus by skilled operators and all mice in a cage were bled within 2 min to avoid handling-induced increases in GCs levels (Pruett *et al.*, 1999). Samples were then centrifuged at $2000 \times g$ at 4°C for 15 min and sera were stored at −80°C until analysis. Spleen and thymus were immediately removed following sacrifice, and these organs were weighed and divided into three portions. One third was fixed in 10% neutral buffered formalin for histological examination. Another section was immediately frozen in liquid nitrogen and stored at −80°C until used for RNA isolation. The remainder was used for cell preparation. All experimental manipulations were undertaken in accordance with the Institutional Guidelines for the Care and Use of Laboratory Animals.

Monoclonal antibodies and reagents. The following monoclonal antibodies (mAbs) were purchased from BD Biosciences PharMingen (San Diego, CA): Fluorescein isothiocyanate (FITC)-conjugated anti-mouse CD4 mAb (RM4-5; rat IgG2a), phycoerythrin (PE)-labeled anti-mouse CD8α mAb (53-6.7; rat IgG2a), FITC-labeled anti-mouse CD11c mAb, PE-conjugated anti-mouse F4/80 mAb (BM8), PE-conjugated anti-mouse TCR mAb, and FITC-labeled anti-mouse CD49b mAb. Rat anti-mouse FcR mAb (2.4G2, IgG2b) was produced by the 2.4G2 hybridoma (ATCC, Rockville, MD) in our laboratory. In addition, PFNA (CAS number: 375-95-1, 97% purity) was purchased from

Sigma Aldrich. Concanavalin A (ConA) was purchased from Sigma Chemical Co. (St Louis, MO). Cells were cultured in RPMI 1640 (GiBco, CA) containing 10% fetal bovine serum, 25mM N'-a-hydroxythylpiperazine-N'-ethanesulfanic acid (Hepes), 2mM L-glutamine, 100 IU/ml of penicillin, 100 μg/ml streptomycin, and 50μM 2-mercaptoethanol (Sigma). The 3-(4,5-dimethyl-thiazol-2-yl)-2-5-diphenyl tetrazolium bromide (MTT) (Sigma Chemical Co.) was dissolved in phosphate-buffered saline (PBS) at a concentration of 5 mg/ml and filtered through a 0.22-μm filter to sterilize and remove insoluble residues.

Cell preparation. Following harvest of the thymus and spleen, single-cell suspensions were prepared by grinding tissue sections with the plunger of a 5-ml disposable syringe followed by suspension in RPMI 1640 medium. Splenocytes were treated with a hemolysis buffer (17mM Tris-HCl and 140mM NH_4Cl, pH 7.2) to remove red blood cells.

Immunofluorescence staining and flow cytometric analysis. Briefly, 5×10^5 splenocytes or thymocytes were washed once with fluorescein activated cell sorter (FACS) buffer (PBS, pH 7.2, containing 0.1% NaN_3 and 0.5% bovine serum albumin [BSA]). Cells were incubated with 2.4G2 to block FcRs and then incubated with an optimal concentration of fluorochrome-labeled specific mAbs for 30 min at 4°C in the dark. At least 10,000 cells were assayed by a FACSCalibur flow cytometry (Becton Dickinson, CA), and data were analyzed with CellQuest software (Becton Dickinson, Mountain View, CA). Nonviable cells were excluded using the vital nucleic acid stain propidium iodide (PI; Sigma). The percentage of cells stained with a particular reagent or reagents was determined by subtracting the percentage of cells stained nonspecifically with the negative control mAb from staining in the same dot-plot region with the anti-mouse mAbs. Molecule expression levels were determined as the median fluorescence intensity of the cells positively stained with the specific mAb.

Cell cycle analysis. Cells were collected and fixed overnight in 70% ethanol at 4°C. Cells were then washed twice with complete PBS and stained with 50 μg/ml PI in the presence of 100 μg/ml DNAse-free RNAse (Sigma). After 30 min at room temperature in the dark, the cells were analyzed using a FACSCalibur flow cytometer (Becton Dickinson). Data were analyzed with CellQuest software (Becton Dickinson).

ConA stimulation and MTT assay. Splenocytes (2×10^6 cells/ml) were stimulated with ConA (2.5 μg/ml) in a 96-well plate (Costar, MA) and incubated at 37°C in 5% CO_2 for 72 h. Cell monolayers in exponential growth were harvested, and 5×10^3 cells were added to each well of a 96-well plate (Nunclon, VWR International, Inc., MD) in a total volume of 100 μl. The plates were incubated for 24 h at 37°C in 5% CO_2. The medium was discarded, and 200 μl of the test extracts for each sample were added to the wells at different concentrations. After a 72-h incubation, 20 μl of the MTT solution was added to each well, and the plates were incubated again for 4 h at 37°C. Following incubation, the medium was discarded, and 100 μl of dimethyl sulfoxide was added to dissolve the formazan crystals. The plate was shaken for 30 min to dissolve the crystal, and the absorbance was measured at 570 nm with a microplate reader. Assays for each concentration were done in triplicate.

Histological analysis. Samples were fixed in 10% neutral buffered formalin for histologic evaluation. Paraffin-embedded tissue sections were cut and stained with hematoxylin and eosin for morphological evaluation.

Hormone and cytokines analysis. Corticosterone is the predominant GC produced in mice, **whereas** the serum cortisol level in murine also reflects the HPA axis function (Bhat *et al.*, 2007; Nakano, 2007). In the present study, the concentrations of adrenocorticotrophic hormone (ACTH) and cortisol in sera samples were measured by enzyme-linked immunosorbent assay (ELISA) according to the manufacturer's directions (RapidBio Lab, CA). Twenty microlitres of serum was required to evaluate cortisol level according to the kit. Absorbance was measured with an ELISA plate reader (Multiskan Ex Primary EIA V. 2.3, Labsystems, MA) at 450 nm. Interleukin (IL)-4 and interferon-gamma (IFN)-γ were measured in 10% homogenates from frozen spleen tissue by

TABLE 1
Sequences of Primers Used for Real-Time RT-PCR Amplification

Target gene	GenBank accession no.	$5' \rightarrow 3'$ Primer sequences	Product length (bp)	T_m (°C)
PPAR-α	NM_001113418	FW: AGATCGGCCTGGCCTTCTAAACATA RW: TGCGTCGGACTCGGTCTTCTTGAT	205	65.0
PPAR-γ	NM_011146	FW: TCCGAAGAACCATCCGATTGAA RW: GCAAGGCACTTCTGAAACCGACA	112	65.0
IL-1β	NM_008361.3	FW: AGCACCTCACAAGCAGAGCACAA RW: CCCTGGGGAAGGCATTAGAAAC	130	65.0
IκBα	NM 010907	FW: ACTTGGTGACTTTGGGTGCTGATGT RW: TGACATCAGCCCCACATTTCAACAA	129	65.0
IKK	NM_010546	FW: TTGCTGCCCAAGGTAGAAGAGGTAG RW: AGGCACTGGAAGGCTGGGACATTAG	211	65.0
GR	NM 008173.3	FW: TTACCCCTACCCTGGTGTCACTGCT RW: TGGTATCGCCTTTGCCCATTTCACT	164	65.0
β-Actin	AK167825	FW: TTCTTGGGTATGGAATCCTGTGGCA RW: CATCCTGTCAGCAATGCCTGGGTAC	144	65.0

Note. FW, forward primer; RW, reverse primer.

ELISA in accordance with the manufacturer's directions (Biosource International, Camarillo, CA). Absorbance was measured with an ELISA plate reader (Multiskan Ex Primary EIA V. 2.3) at wavelengths of 450 and 492 nm, respectively.

Real-time reverse transcription–PCR analysis. RNA was isolated from individual mouse thymus samples using the RNeasy mini RNA isolation protocol (Qiagen, Hilden, Germany). The concentration of total RNA was measured by absorbance at 260 nm using a UV1240 spectrophotometer (Shimadzu, Japan). The purity was estimated by the 260/280 nm absorbance ratio. One microgram of total RNA was subjected to reverse transcription using an oligo-$(dT)_{15}$ primer (Promega, WI) and M-MuLV reverse transcriptase (New England Biolabs, UK) according to the manufacturers' instructions. The samples were incubated for 60 min at 37°C to facilitate reverse transcription and then incubated for 5 min at 95°C. Real-time PCR reactions were performed with the Stratagene Mx3000P qPCR system (Stratagene, CA). For quantification of gene expression, SYBR Green PCR Master Mix reagent kits (Takala, Dalian, China) were used according to the manufacturer's instructions. Mouse-specific primers were designed for the genes of interest: PPAR-α, PPAR-γ, IκBα kinase (IKK), the inhibitory protein IκBα, glucocorticoid receptor (GR), and IL-1β (Table 1). The housekeeping gene β-actin was used as an internal control. The differences of efficiencies in amplification between the target genes and β-actin were all less than 5%. The PCR amplification protocol was 95°C for 15 min followed by 40 cycles of 94°C for 5 s, 65°C for 20 s, and 72°C for 30 s. After PCR, a melting curve analysis was performed to demonstrate the specificity of the PCR product, which was displayed as a single peak (data not shown). Each sample was analyzed in triplicate. The relative expression ratio (R) of a target gene is expressed for the sample versus the control in comparison to the β-actin gene. R is calculated based on the following equation (Livak and Schmittgen, 2001): $R = 2^{-\Delta\Delta C_t}$, where C_t represents the cycle number at which the fluorescence signal is first significantly different from background and $\Delta\Delta C_t$ is

$$\left(C_{t,target} - C_{t,actin}\right)_{treatment} - \left(C_{t,target} - C_{t,actin}\right)_{control}.$$

Statistical analysis. Data were analyzed using SPSS for Windows 13.0 Software (SPSS, Inc., Chicago, IL) and presented as means with standard errors (mean ± SE). Differences between the control and the treatment groups were determined using a one-way ANOVA followed by the Duncan's multiple range test. A p value of < 0.05 was considered statistically significant.

RESULTS

Effect of PFNA Exposure on Body Weight

No significant change was observed following exposure of mice to 1 mg PFNA/kg/day compared with controls (Table 2). For mice exposed to 3 mg PFNA/kg/day, significant decreases in mean body weight (reduced by 12.6% compared with controls, $p < 0.01$) and body weight gain were observed at day 14, whereas mice exposed to 5 mg PFNA/kg/day exhibited significantly decreased body weight (reduced by 13.6%, $p < 0.01$) and body weight gain as early as test day 7 and even more severe decreases (reduced by 15.7%, $p < 0.01$) at the end of study.

Effect of PFNA Exposure on Thymus

Absolute thymus weights were significantly reduced by 33.3% and 44.4% at doses of 3 and 5 mg PFNA/kg/day, respectively, after 14 days exposure to PFNA ($p < 0.01$). Relative thymus weights were also markedly decreased in both groups (Fig. 1A). Although no histopathological changes were observed by optical microscope in thymi after PFNA treatment (data not shown), the percentages of different T-cell subsets were significantly altered as determined by cell surface phenotype analysis. $CD4^+CD8^+$ cells were reduced by 42% in mice receiving the highest dose of PFNA, whereas the proportions of $CD4^+CD8^-$ and $CD4^-CD8^+$ cells were correspondingly increased (Fig. 1B). To further examine the cell cycle and apoptosis of thymocytes, flow cytometry to detect PI binding to DNA was used. Upon administration of 5 mg PFNA/kg/day to mice for 14 days, significant decreases in the proportion of thymocytes in the S and G2/M phases concurrently with a significant increase in the G0/G1 phase were observed. In addition, the percentage of G2/M phase cells was also dramatically decreased in mice receiving 3 mg PFNA/kg/day (Fig. 1C). Apoptosis was increased

TABLE 2
### Body Weight and Weight Gain of Mice Treated with PFNA for 14 Days

Dose (mg/kg/day)	0	1	3	5
Body weight at day 0 (g)	19.7 ± 3.5	19.3 ± 3.2	19.8 ± 2.8	19.8 ± 2.2
Body weight at day 7 (g)	19.6 ± 3.4	19.3 ± 2.3	19.1 ± 2.2	17.1 ± 2.6**
Body weight at day 14 (g)	20.3 ± 2.9	19.2 ± 3.0	17.3 ± 2.8**	16.7 ± 1.7**
Total weight gain during the 14 days (g)	0.6 ± 0.2	−0.1 ± 0.1	−2.5 ± 0.9**	−3.1 ± 1.6**

Note. Data are shown as mean ± SE from six mice per group. A significant difference from the control is indicated as *$p < 0.05$ and **$p < 0.01$.

significantly in thymocytes from mice receiving 5 mg PFNA/kg/day compared with the control (Fig. 1D). Both cell cycle arrest at the G0/G1 phase, which prevented thymocyte proliferation, and increased apoptosis contributed to the observed thymic atrophy.

Effects of PFNA Exposure on Spleen

The absolute spleen weights were significantly reduced by 9.6% and 12.7% in the two higher doses of PFNA-treated groups ($p < 0.01$), and the relative spleen weights were markedly decreased in mice receiving 5 mg PFNA/kg/day (Fig. 2A). No obvious changes in the spleen red pulp or white pulp were noted, and no infiltration of mononuclear inflammatory cells was observed. The spleen capsule was crinkled (data not shown), which may be a result of splenatrophy. Cell surface phenotype analysis indicated a significant decrease in the percentages of F4/80^{+} and CD49b^{+} cells in all of the treatment groups and of CD11c^{+} in the 3 and 5 mg PFNA/kg/day groups. Thus, the innate immune cells in the spleen were damaged following PFNA treatment. The percentages of CD4^{+} and TCR^{+} cells in the spleen were not altered, whereas the percentage of CD8^{+} cells was decreased in the 1 mg PFNA/kg/day animals ($p < 0.05$; Fig. 2B). Analysis of the cell cycle and apoptosis revealed a trend similar to that
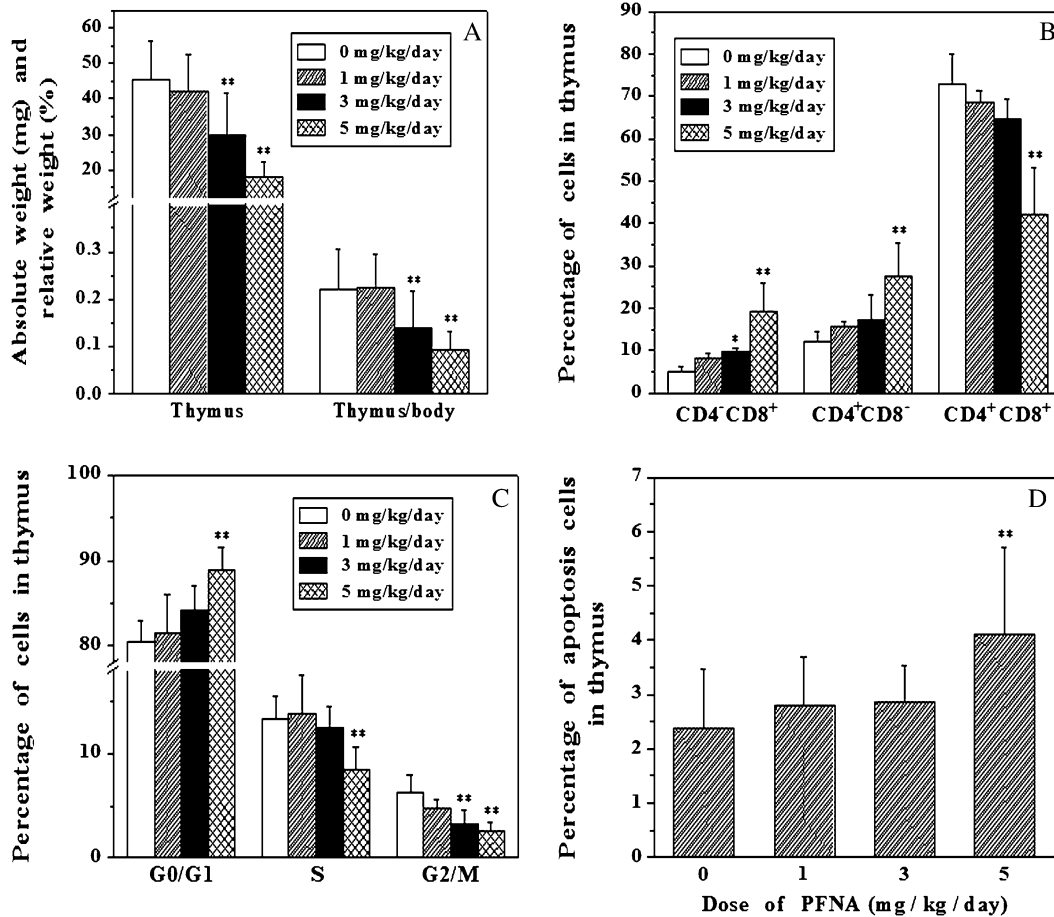
FIG. 1. (A) Absolute weight and relative weight of thymi from control and PFNA-exposed male mice. (B) Percentages of T-cell subsets in thymus from control and PFNA-exposed male mice. (C) Percentages of thymocytes in different phases of cell cycle from control and PFNA-exposed male mice. (D) Percentages of apoptosis cells in thymus from control and PFNA-exposed male mice. For all panels, the values are presented as the mean ± SE for six mice per group. *$p < 0.05$; **$p < 0.01$.
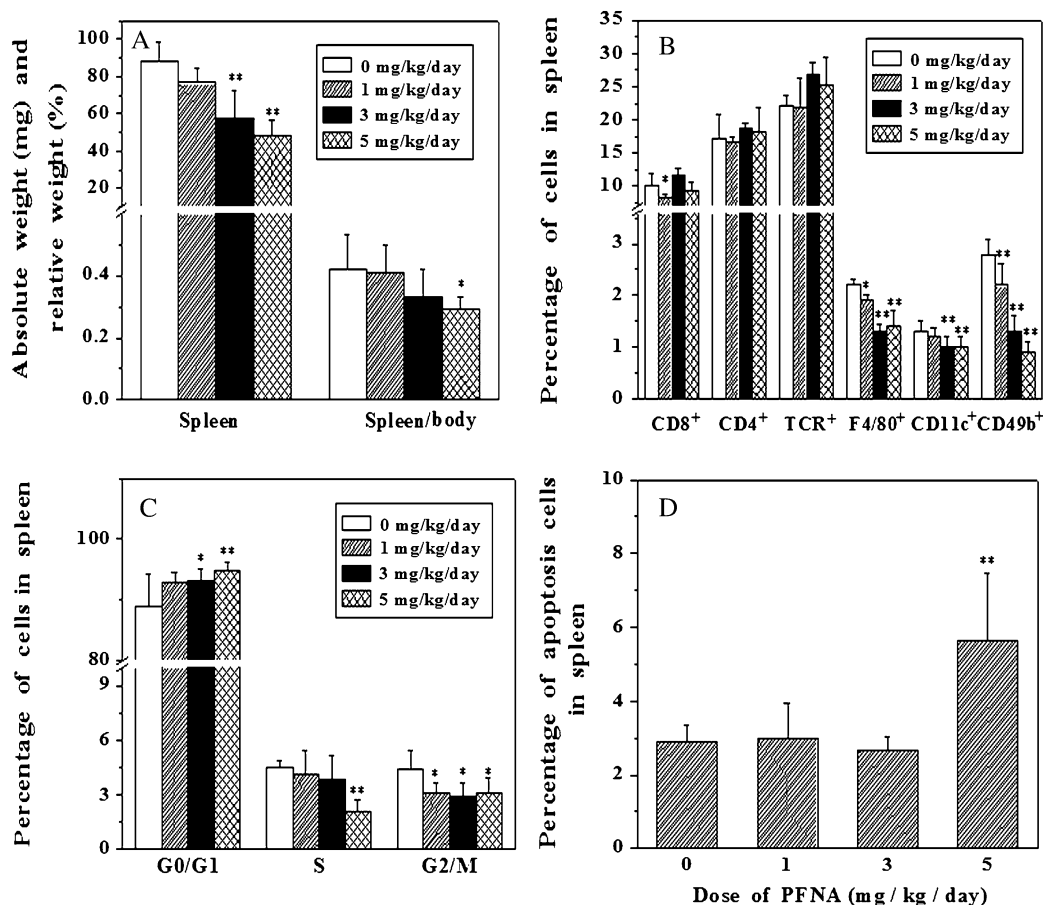
FIG. 2. (A) Absolute weight and relative weight of spleens from control and PFNA-exposed male mice. (B) Percentages of splenic cell subsets from control and PFNA-exposed male mice. (C) Percentages of splenocytes in different phases of cell cycle from control and PFNA-exposed male mice. (D) Percentages of apoptotic cells in the spleens from control and PFNA-exposed male mice. For all panels, the data are presented as the mean ± SE for six mice per group. $*p < 0.05$; $**p < 0.01$.

observed in the thymus, with the S-phase cells decreased and the G0/G1-phase cells increased in the 5 mg PFNA/kg/day group compared with the control (Fig. 2C). A significant decrease of cells in the G2/M phase occurred in all treatment groups (Fig. 2C). Splenocyte apoptosis was increased significantly in mice receiving 5 mg PFNA/kg/day compared with the control (Fig. 2D). These results were similar to those from a previous study on male C57BL/6 mice treated with PFOA (Yang *et al.*, 2001), and thus, this increase in apoptosis may explain the splenic atrophy.

To further test whether PFNA exposure influenced the response of splenic T lymphocytes to an *in vitro* stimuli, spleen cells were incubated overnight with the T-cell mitogen ConA. No obvious differences in ConA-induced splenic T lymphocyte blastogenesis were observed between the control and the PFNA-treated groups (data not shown). This finding is consistent with previous study in which adult male and female B6C3F1 mice were exposed to PFOS (0–5 mg/kg total administered dose) (Peden-Adams *et al.*, 2008).

Having observed no significant alteration in the splenic T-cell proliferation response, we next examined whether PFNA

exposure influences the secretion of cytokines by T lymphocytes. Spleen cells from PFNA-treated mice produced significantly lower quantities of IL-4, whereas the quantity of IFN-γ was significantly decreased only in mice exposed to 5 mg PFNA/kg/day (Fig. 3).

Hormone Analysis

The concentrations of ACTH and cortisol in sera samples were measured by ELISA to test whether the HPA axis was affected by PFNA treatment. The levels of ACTH and cortisol were significantly increased by 53% and 51%, respectively, at the highest dose compared with the control ($p < 0.01$; Fig. 4). The nearly synchronous changes of ACTH and cortisol in this process implicated the activation of the HPA axis, which may be involved in the immunomodulation by PFNA.

Gene Expression

Real-time reverse transcription–PCR (RT-PCR) showed that the mRNA levels of both PPAR-α and PPAR-γ were significantly increased (6.1-fold and 2.6-fold, respectively) in
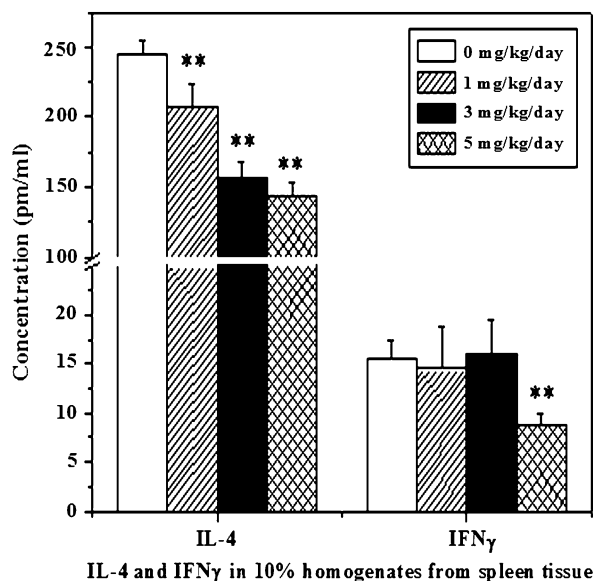
FIG. 3. Concentrations of IL-4 and IFN-γ in 10% homogenates from the spleens of control and PFNA-exposed male mice. Values are presented as the mean ± SE for six mice per group. *$p < 0.05$; **$p < 0.01$.

the 1 mg PFNA/kg/day group compared with the control ($p < 0.01$; Figs. 5A, B). Despite the increased levels of cortisol in the sera, the expression of GR in the thymus did not exhibit a significant change in any of the treated groups compared with the control (Fig. 5C). No significant changes were observed in the expression of IKK or IκBα, which are genes involved in the NF-κB–signaling pathway, in animals from any of the
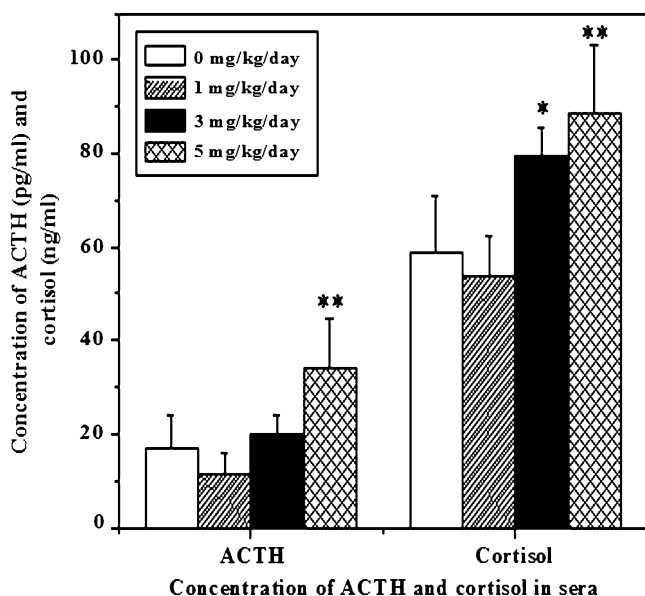

FIG. 4. Concentrations of cortisol and ACTH in the serum from control and PFNA-exposed male mice. Values are presented as the mean ± SE for six mice per group. *$p < 0.05$; **$p < 0.01$.

treatment groups (Fig. 5D, 5E). On the other hand, IL-1β, a target gene of the NF-κB–signaling pathway, was significantly increased 3-fold in the 1 mg PFNA/kg/day group compared with the control ($p < 0.01$; Fig. 5F).

DISCUSSION

Current data supports an effect of environmental chemicals on the immune response. Here, we demonstrated that oral administration of PFNA (3 and 5 mg PFNA/kg/day) to mice for fourteen days resulted in a significant reduction of body weight as well as of thymus and spleen weights. The atrophy of the lymphoid organs in the higher dose groups may be explained by the impairment of cell cycle progression and increased apoptosis. The phenotypic analysis of thymocytes and splenocytes demonstrated that the percentage of CD4$^+$CD8$^+$ thymocytes in the thymus was reduced most dramatically following administration of 5 mg PFNA/kg/day. The more pronounced effect on this double positive cell subset suggested that PFNA may interfere with the process of thymocyte maturation and differentiation. The significant decrease in the proportions of thymocytes present in the S and G2/M phases further supported this hypothesis. The results were similar to previous studies on PFOA-treated mice (Yang *et al.*, 2000, 2001). In the spleen, the innate immune cells seemed to be the important cellular targets of PFNA, with a significant decrease in the percentages of F4/80$^+$ and CD49b$^+$ cells in all treated groups and of CD11c$^+$ cells in the 3 and 5 mg PFNA/kg/day groups. The percentages of T-cell subsets in the spleen, however, were nearly unchanged following PFNA treatment. In addition, no obvious differences in ConA-induced splenic T lymphocyte blastogenesis were observed between the control and the PFNA-treated groups. This finding was consistent with the previous study of PFOS (0-5 mg/kg total administered dose) exposure in adult male and female B6C3F1 mice (Peden-Adams *et al.*, 2008) and was also similar to the exposure of sulfluramid in mice (Peden-Adams *et al.*, 2007). On the other hand, PFOA exposure at a dietary concentration of 0.02% for ten days in mice decreased both T- and B-cell mitogen-induced lymphoproliferation (Yang *et al.*, 2002). This discrepancy may be directly related to differences in effects between the classes of PFCs.

To further examine the effects of PFNA on the function of splenic lymphocytes, production of cytokines in the spleen was quantified. IFN-γ is characteristic of T helper 1 cells, and IL-4 is the signature cytokine of T helper 2 cells. Both cytokines play vital roles in the immune response and are thus useful for the evaluation of immune function. Significant reductions in IFN-γ (at the dose of 5 mg PFNA/kg/day) and IL-4 (at all doses of PFNA) were observed. Although no change in T lymphocyte blastogenesis was observed, these results indicated that PFNA exerts a profound effect on the secretion of cytokines, especially IL-4, by T lymphocytes. Alteration of these
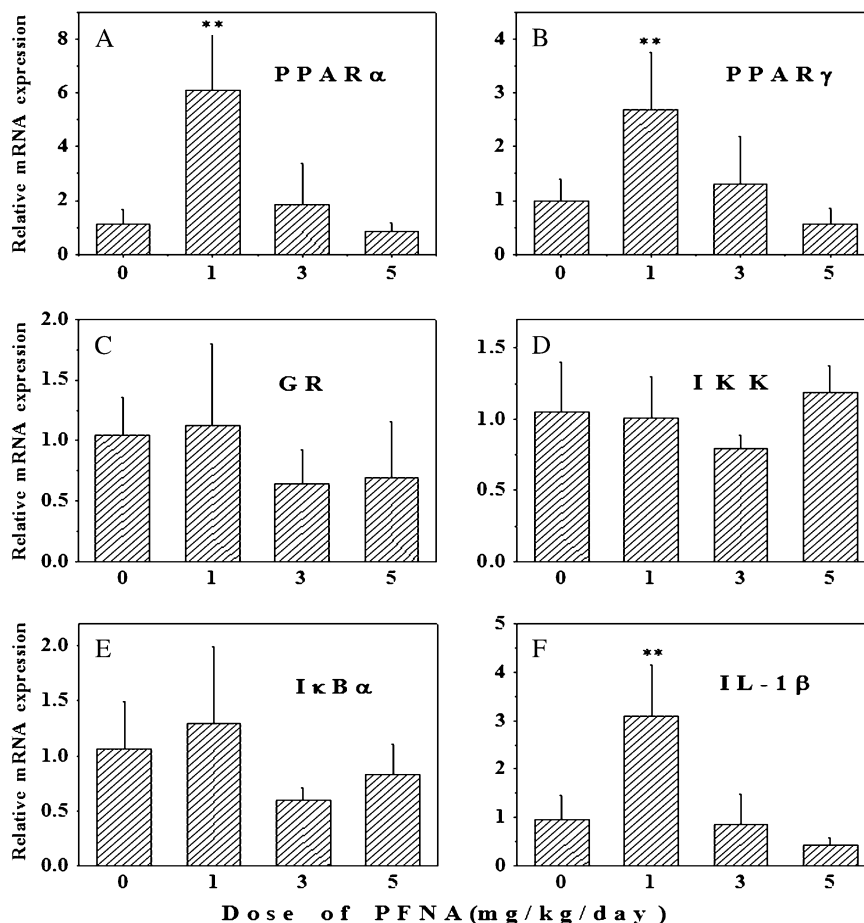
FIG. 5. Real-time quantitative RT-PCR analyses of thymus mRNA expression levels of (A) PPAR-α, (B) PPAR-γ, (C) GR, (D) IKK, (E) IκBα, and (F) IL-1β from control and PFNA-exposed male mice. Gene expression levels represent the relative mRNA expression compared with the controls. Values are given as the mean ± SE for six mice per group. *$p < 0.05$; **$p < 0.01$.

cytokines may subsequently impair the immune function of lymphocytes.

Previous studies have indicated that PPAR-α is the most likely target of PFCs in liver in mice (Abbott *et al.*, 2007; Vanden Heuvel *et al.*, 2006), and exposure to some PFCs activates PPAR-γ to a certain extent (Vanden Heuvel *et al.*, 2006; Zhang *et al.*, 2008). Ligand-induced activation of PPAR-α or PPAR-γ has been shown to influence the differentiation of thymocytes, induce lymphoid organ atrophy, induce lymphocyte apoptosis, suppress innate immune cell activity (Chung *et al.*, 2003; Cunard *et al.*, 2002b, 2004), and inhibit the production of IFN-γ, tumor necrosis factor-α, IL-2, and IL-4 in T cells (Cunard *et al.*, 2002a; Lovett-Racke *et al.*, 2004). PFNA has been reported to be a more potent agonist of PPAR-α than other PFCs, such as perfluoroheptanoic acid, perfluorohexanoic acid, and PFOA (Kudo, 2006), but whether PFNA activates PPAR-γ is not known. Our findings showed that PPAR-α and PPAR-γ mRNA were upregulated significantly in the thymus of mice receiving 1 mg PFNA/kg/day, whereas the expression of both genes was unchanged in the thymi of mice

receiving 3 or 5 mg PFNA/kg/day. This result suggests that the maximum transcriptional activity of PPAR-α may be following administration of 1 mg PFNA/kg/day in mice, and this conclusion parallels the maximal transcriptional activity of PPAR-α at 1 mg perfluorododecanoic acid/kg/day observed in rats on day 14 (Zhang *et al.*, 2008). In other studies, 10μM PFOA induced the maximal transcriptional activity of PPAR-α in mice (Maloney and Waxman, 1999). The significant upregulation of PPAR-α and PPAR-γ may, to some extent, explain the immunotoxicity observed at this dosage.

Severe immunotoxicity was observed in the 3 and 5 mg PFNA/kg/day treatment groups despite the unchanged expression of PPAR-α and PPAR-γ. Thus, a PPAR-α–independent mechanism is likely at play. A previous study on the immunomodulatory effects of PFOA in mice also revealed a PPAR-α–independent mechanism (Yang *et al.*, 2002). Due to their fatty acid structure, PFCs are hypothesized to act as structural mimics of fatty acids in organisms (Vanden Heuvel *et al.*, 2006). Fatty acids can activate the HPA axis and intervene in inflammatory conditions and immunomodulation

in rodents (Song, 2005). Therefore, the activation of the HPA axis and the subsequent increase in ACTH and cortisol levels in sera in the groups receiving the higher dose of PFNA was not surprising. Endogenous or synthetic GCs have been shown to induce thymocyte apoptosis preferentially in the $CD4^+CD8^+$ compartment (Boldizsár *et al.*, 2006) as well as to induce cell cycle arrest in G0/G1 (Reisman and Thompson, 1995). In addition, higher levels of GCs were reported to suppress innate immune responses (Liberman *et al.*, 2007). More specifically, high GC levels attenuate Langerhans cell/ dendritic cell maturation and function (Elftman *et al.*, 2007), reduce the percentage phagocytosis and the phagocytic index (Bishayi and Ghosh, 2007), and induce apoptosis in mouse natural killer cells (Migliorati *et al.*, 1994). In the 3 and 5 mg PFNA/kg/day treatment groups, increased cortisol levels were associated with remarkable induction of lymphocyte apoptosis, G0/G1 arrest, and a decreased $CD4^+CD8^+$ subset in the thymus, which led to significant atrophy of the organ. At the same time, the significant decrease in innate immune cells in the higher dose groups may also be attributed to the increased cortisol levels.

The majority of the biological effects of GCs are mediated by the GR via activation and repression of gene expression. Real-time RT-PCR showed no alteration of GR expression in the thymus of mice from all PFNA-treated groups, despite the significant increases of cortisol levels in the sera from mice receiving the higher doses of PFNA. Thus, the non-transcription GR mechanisms that were previously described in studies of thymocytes in BALB/c mice after GC analogue administration are favored (Boldizsár *et al.*, 2006). The effect of GC on immunomodulation in current study, therefore, occurred either via regulation of GR at the protein level or via other indirection ways, such as regulation of transcription factor signaling pathways.

Among the known transcription factor signaling pathways, the NF-κB–signaling pathway plays an important role in the modulation of inflammatory and immune response (Delerive *et al.*, 2000; Smoak and Cidlowski, 2004; Sung *et al.*, 2006). In most nonactivated cells, NF-κB remains in the cytoplasm as an inactive complex through its association with the inhibitory protein IκBα (Baeuerle and Baltimore, 1996). Dimeric IKK complex phosphorylates IκBα and leads to subsequent ubiquitination and degradation of IκBα and then release of the NF-κB protein (Baeuerle and Baltimore, 1996). Free NF-κB dimers translocate to the nucleus to regulate target gene transcription. GC and PPAR ligands upregulate the expression of IκBα in mice and other animals (Almawi and Melemedjian, 2002; Dehmer *et al.*, 2004; Delerive *et al.*, 2000; Scheinman *et al.*, 1995). The significant increase of PPARs expression at the lower doses of PFNA and the increased cortisol level at higher doses of PFNA suggested that the NF-κB–signaling pathway may be involved in the process of immunotoxicity; however, neither IKK nor IκBα mRNA was altered in any PFNA-treated groups. Furthermore, IL-1β, one of the NF-κB target genes,

was significantly increased in mice receiving 1 mg PFNA/kg/ day. Together, these results suggest that PFNA exposure did not suppress the NF-κB–signaling pathway at the transcriptional level. Further investigation is necessary to clarify whether the NF-κB–signaling pathway is regulated at the post-transcriptional level and whether other transcription factors, such as AP-1, are impacted following PFNA treatment.

In conclusion, our results demonstrate the immunotoxicity of PFNA on lymphoid organs and lymphocyte homeostasis in BALB/c mice. In addition, PFNA impaired secretion of cytokines by lymphocytes, and this impairment may effectively weaken the immune function of mice. Significant upregulation of PPAR-α and PPAR-γ mRNA may contribute to the immunotoxicity observed in the 1 mg PFNA/kg/day treatment group. In the 3 and 5 mg PFNA/kg/day treatment groups, PFNA activated the HPA axis and resulted in increased ACTH and cortisol levels in the sera of the mice. Therefore, activation of PPAR and the HPA axis may be involved in the immunotoxicity of PFNA in mice. Surprisingly, at the transcriptional level, the NF-κB–signaling pathway did not contribute to the immunotoxicity by this chemical. Further immunotoxicity studies are required to understand the mechanisms of immunomodulation of PFNA and to determine potential health risks associated with exposure to this chemical.

FUNDING

REFERENCES

Abbott, B. D., Wolf, C. J., Schmid, J. E., Das, K. P., Zehr, R. D., Helfant, L., Nakayama, S., Lindstrom, A. B., Strynar, M. J., and Lau, C. (2007). Perfluorooctanoic acid induced developmental toxicity in the mouse is dependent on expression of peroxisome proliferator activated receptor-alpha. *Toxicol. Sci.* **98,** 571–581.

Almawi, W. Y., and Melemedjian, O. K. (2002). Negative regulation of nuclear factor-kappaB activation and function by glucocorticoids. *J. Mol. Endocrinol.* **28,** 69–78.

Baeuerle, P. A., and Baltimore, D. (1996). NF-kappa B: Ten years after. *Cell* **87,** 13–20.

Bhat, M. S., Rao, G., Murthy, K. D., and Bhat, P. G. (2007). Housing in pyramid counteracts neuroendocrine and oxidative stress caused by chronic restraint in rats. *Evid. Based Complement Alternat. Med.* **4,** 35–42.

Bishayi, B., and Ghosh, S. (2007). Immunobiological changes of in vivo glucocorticoid depleted male Swiss albino rats. *Immunobiology* **212,** 19–27.

Boldizsár, F., Pálinkás, L., Czömpöly, T., Bartis, D., Németh, P., and Berki, T. (2006). Low glucocorticoid receptor (GR), high Dig2 and low Bcl-2 expression in double positive thymocytes of BALB/c mice indicates their endogenous glucocorticoid hormone exposure. *Immunobiology* **211,** 785–796.

Chen, X., Li, M., Sun, W., Bi, Y., Cai, M., Liang, H., Yu, Q., He, X., and Weng, J. (2008). Peroxisome proliferator-activated receptor alpha agonist-induced down-regulation of hepatic glucocorticoid receptor expression in SD rats. *Biochem. Biophys. Res. Commun.* **368,** 865–870.

Chung, S. W., Kang, B. Y., and Kim, T. S. (2003). Inhibition of interleukin-4 production in $CD4^+$ T cells by peroxisome proliferator-activated receptor-gamma

(PPAR-gamma) ligands: Involvement of physical association between PPAR-gamma and the nuclear factor of activated T cells transcription factor. *Mol. Pharmacol.* **64,** 1169–1179.

Cunard, R., DiCampli, D., Archer, D. C., Stevenson, J. L., Ricote, M., Glass, C. K., and Kelly, C. J. (2002b). WY14,643, a PPAR alpha ligand, has profound effects on immune responses in vivo. *J. Immunol.* **169,** 6806–6812.

Cunard, R., Eto, Y., Muljadi, J. T., Glass, C. K., Kelly, C. J., and Ricote, M. (2004). Repression of IFN-gamma expression by peroxisome proliferator-activated receptor gamma. *J. Immunol.* **172,** 7530–7536.

Cunard, R., Ricote, M., DiCampli, D., Archer, D. C., Kahn, D. A., Glass, C. K., and Kelly, C. J. (2002a). Regulation of cytokine expression by ligands of peroxisome proliferator activated receptors. *J. Immunol.* **168,** 2795–2802.

Dehmer, T., Heneka, M. T., Sastre, M., Dichgans, J., and Schulz, J. B. (2004). Protection by pioglitazone in the MPTP model of Parkinson's disease correlates with I kappa B alpha induction and block of NF kappa B and iNOS activation. *J. Neurochem.* **88,** 494–501.

Delerive, P., Gervois, P., Fruchart, J. C., and Staels, B. (2000). Induction of IkappaBalpha expression as a mechanism contributing to the anti-inflammatory activities of peroxisome proliferator-activated receptor-alpha activators. *J. Biol. Chem.* **275,** 36703–36707.

DeWitt, J. C., Copeland, C. B., Strynar, M. J., and Luebke, R. W. (2008). Perfluorooctanoic acid induced immunomodulation in adult C57BL/6J or C57BL/6N female mice. *Environ. Health Perspect.* **116,** 644–650.

Elftman, M. D., Norbury, C. C., Bonneau, R. H., and Truckenmiller, M. E. (2007). Corticosterone impairs dendritic cell maturation and function. *Immunology* **122,** 279–290.

Ellis, D. A., Martin, J. W., De Silva, A. O., Mabury, S. A., Hurley, M. D., Andersen, M. P. S., and Wallington, T. J. (2004). Degradation of fluorotelomer alcohol; A likely atmospheric source of perfluorinated carboxylic acids. *Environ. Sci. Technol.* **38,** 3316–3321.

Giesy, J. P., and Kannan, K. (2002). Perfluorochemical surfactants in the environment. *Environ. Sci. Technol.* **36,** 146A–152A.

Guruge, K. S., Taniyasu, S., Yamashita, N., Wijeratna, S., Mohotti, K. M., Seneviratne, H. R., Kannan, K., Yamanaka, N., and Miyazaki, S. (2005). Perfluorinated organic compounds in human blood serum and seminal plasma: A study of urban and rural tea worker populations in Sri Lanka. *J. Environ. Monit.* **7,** 371–377.

Haukas, M., Berger, U., Hop, H., Gulliksen, B., and Gabrielsen, G. W. (2007). Bioaccumulation of per- and polyfluorinated alkyl substances (PFAS) in selected species from the Barents Sea food web. *Environ. Pollut.* **148,** 360–371.

Houde, M., Martin, J. W., Letcher, R. J., Solomon, K. R., and Muir, D. C. (2006). Biological monitoring of polyfluoroalkyl substances: A review. *Environ. Sci. Technol.* **40,** 3463–3473.

Ialenti, A., Grassia, G., Di Meglio, P., Maffia, P., Di Rosa, M., and Ianaro, A. (2005). Mechanism of the anti-inflammatory effect of thiazolidinediones: Relationship with the glucocorticoid pathway. *Mol. Pharmacol.* **67,** 1620–1628.

Jondal, M., Pazirandeh, A., and Okret, S. (2004). Different roles for glucocorticoids in thymocyte homeostasis? *Trends. Immunol.* **25,** 595–600.

Kleszczyński, K., Gardzielewski, P., Mulkiewicz, E., Stepnowski, P., and Składanowski, A. C. (2007). Analysis of structure-cytotoxicity in vitro relationship (SAR) for perfluorinated carboxylic acids. *Toxicol. In Vitro* **21,** 1206–1211.

Kudo, N., Suzuki-Nakajima, E., Mitsumoto, A., and Kawashima, Y. (2006). Responses of the liver to perfluorinated fatty acids with different carbon chain length in male and female mice: In relation to induction of hepatomegaly, peroxisomal beta-oxidation and microsomal 1-acylglycerophosphocholine acyltransferase. *Biol. Pharm. Bull.* **29,** 1952–1957.

Lau, C., Anitole, K., Hodes, C., Lai, D., Pfahles-Hutchens, A., and Seed, J. (2007). Perfluoroalkyl acids: A review of monitoring and toxicological findings. *Toxicol. Sci.* **99,** 366–394.

Liberman, A. C., Druker, J., Perone, M. J., and Arzt, E. (2007). Glucocorticoids in the regulation of transcription factors that control cytokine synthesis. *Cytokine Growth Factor Rev.* **18,** 45–56.

Livak, K. J., and Schmittgen, T. D. (2001). Analysis of relative gene expression data using real-time quantitative PCR and the $2-\Delta\Delta Ct$ method. *Methods* **25,** 402–408.

Love, O. P., Shutt, L. J., Silfies, J. S., Bortolotti, G. R., Smits, J. E., and Bird, D. M. (2003). Effects of dietary PCB exposure on adrenocortical function in captive American kestrels (*Falco sparverius*). *Ecotoxicology* **12,** 199–208.

Lovett-Racke, A. E., Hussain, R. Z., Northrop, S., Choy, J., Rocchini, A., Matthes, L., Chavis, J. A., Diab, A., Drew, P. D., and Racke, M. K. (2004). Peroxisome proliferator-activated receptor alpha agonists as therapy for autoimmune disease. *J. Immunol.* **172,** 5790–5798.

Maloney, E. K., and Waxman, D. J. (1999). Trans-activation of PPARα and PPARγ by structurally diverse environmental chemicals. *Toxicol. Appl. Pharmacol* **161,** 209–218.

Migliorati, G., Nicoletti, I., Nocentini, G., Pagliacci, M. C., and Riccardi, C. (1994). Dexamethasone and interleukins modulate apoptosis of murine thymocytes and peripheral T-lymphocytes. *Pharmacology* **30,** 43–52.

Nakano, Y. (2007). Effect of chronic topical exposure to low-dose noxious chemicals and stress on skin sensitivity in mice. *J. Occup. Health* **49,** 431–442.

Nelson, D. L., Frazier, D. E., Ericson, J. E., Tarr, M. J., and Mathes, L. E. (1992). The effects of perfluorodecanoic acid (PFDA) on humoral, cellular, and innate immunity in Fischer 344 rats. *Immunopharmacol. Immunotoxicol* **14,** 925–938.

Pabello, N. G., and Lawrence, D. A. (2006). Neuroimmunotoxicology: Modulation of neuroimmune networks by toxicants. *Clin. Neurosci. Res.* **6,** 69–85.

Peden-Adams, M. M., EuDaly, J. G., Dabra, S., EuDaly, A., Heesemann, L., Smythe, J., and Keil, D. E. (2007). Suppression of humoral immunity following exposure to the perfluorinated insecticide sulfluramid. *J. Toxicol. Environ. Health A.* **70,** 1130–1141.

Peden-Adams, M. M., Keller, J. M., Eudaly, J. G., Berger, J., Gilkeson, G. S., and Keil, D. E. (2008). Suppression of humoral immunity in mice following exposure to perfluorooctane sulfonate (PFOS). *Toxicol. Sci.* doi:10.1093/toxsci/kfn059.

Preil, J., Müller, M. B., Gesing, A., Reul, J. M., Sillaber, I., van Gaalen, M. M., Landgrebe, J., Holsboer, F., Stenzel-Poore, M., and Wurst, W. (2001). Regulation of the hypothalamic-pituitary-adrenocortical system in mice deficient for CRH receptors 1 and 2. *Endocrinology* **142,** 4946–4955.

Pruett, S. B., Collier, S., Wu, W. J., and Fan, R. (1999). Quantitative relationships between the suppression of selected immunological parameters and the area under the corticosterone concentration vs. time curve in B6C3F1 mice subjected to exogenous corticosterone or to restraint stress. *Toxicol. Sci.* **49,** 272–280.

Reisman, D., and Thompson, E. A. (1995). Glucocorticoid regulation of cyclin D3 gene transcription and mRNA stability in lymphoid cells. *Mol. Endocrinol.* **9,** 1500–1509.

Rice, D. C., and Hayward, S. (1997). Effects of postnatal exposure to a PCB mixture in monkeys on nonspatial discrimination reversal and delayed alternation performance. *Neurotoxicology* **18,** 479–494.

Ricote, M., Li, A. C., Willson, T. M., Kelly, C. J., and Glass, C. K. (1998). The peroxisome proliferator-activated receptor-gamma is a negative regulator of macrophage activation. *Nature* **391,** 79–82.

Scheinman, R. I., Cogswell, P. C., Lofquist, A. K., and Baldwin, A. S. (1995). Role of transcriptional activation of I kappa B alpha in mediation of immunosuppression by glucocorticoids. *Science* **270,** 283–286.

Shridhar, S., Farley, A., Reid, R. L., Foster, W. G., and Van Vugt, D. A. (2001). The effect of 2,3,7,8-tetrachlorodibenzo-p-dioxin on corticotrophin-releasing hormone, arginine vasopressin, and pro-opiomelanocortin mRNA levels in the hypothalamus of the cynomolgus monkey. *Toxicol. Sci.* **63,** 181–188.

Smoak, K. A., and Cidlowski, J. A. (2004). Mechanisms of glucocorticoid receptor signaling during inflammation. *Mech. Ageing. Dev.* **125,** 697–706.

Song, C. (2005). n-3 Fatty acid EPA alone or in combination with GLA modulate HPA axis activity, inflammation condition, and related gene expressions in a rodent model of depression. *Brain Behav. Immun.* **19,** e43–e74; e66.

Sung, B., Park, S., Yu, B. P., and Chung, H. Y. (2006). Amelioration of age-related inflammation and oxidative stress by PPARgamma activator: Suppression of NF-kappaB by 2,4-thiazolidinedione. *Exp. Gerontol.* **41,** 590–599.

Tugwood, J. D., Issemann, I., Anderson, R. G., Bundell, K. R., McPheat, W. L., and Green, S. (1992). The mouse peroxisome proliferator activated receptor recognizes a response element in the 5' flanking sequence of the rat acyl CoA oxidase gene. *EMBO J.* **11,** 433–439.

Vanden Heuvel, J. P., Thompson, J. T., Frame, S. R., and Gillies, P. J. (2006). Differential activation of nuclear receptors by perfluorinated fatty acid analogs and natural fatty acids: A comparison of human, mouse, and rat peroxisome proliferator-activated receptoralpha, -beta, and -gamma, liver X receptor-beta, and retinoid X receptor-alpha. *Toxicol. Sci.* **92,** 476–489.

Van de Vijver, K. I., Hoff, P., Das, K., Brasseur, S., Van Dongen, W., Esmans, E., Reijnders, P., Blust, R., and De Coen, W. (2005). Tissue distribution of perfluorinated chemicals in harbor seals (*Phoca vitulina*) from the Dutch Wadden Sea. *Environ. Sci. Technol.* **39,** 6978–6984.

Yang, Q., Xie, Y., Alexson, S. E., Nelson, B. D., and DePierre, J. W. (2002). Involvement of the peroxisome proliferator-activated receptor alpha in the immunomodulation caused by peroxisome proliferators in mice. *Biochem. Pharmacol.* **63,** 1893–1900.

Yang, Q., Xie, Y., and DePierre, J. W. (2000). Effects of peroxisome proliferators on the thymus and spleen of mice. *Clin. Exp. Immunol.* **122,** 219–226.

Yang, Q., Xie, Y., Eriksson, A. M., Nelson, B. D., and DePierre, J. W. (2001). Further evidence for the involvement of inhibition of cell proliferation and development in thymic and splenic atrophy induced by the peroxisome proliferator perfluoroctanoic acid in mice. *Biochem. Pharmacol.* **62,** 1133–1140.

Zhang, H., Shi, Z., Liu, Y., Wei, Y., and Dai, J. (2008). Lipid homeostasis and oxidative stress in the liver of male rats exposed to perfluorododecanoic acid. *Toxicol. Appl. Pharmacol.* **227,** 16–25.